Viscoelastic Functionally Graded Finite-Element Method Using Correspondence Principle

Eshan V. Dave, S.M.ASCE[1]; Glaucio H. Paulino, Ph.D., M.ASCE[2]; and
William G. Buttlar, Ph.D., P.E., A.M.ASCE[3]

Abstract: Capability to effectively discretize a problem domain makes the finite-element method an attractive simulation technique for modeling complicated boundary value problems such as asphalt concrete pavements with material non-homogeneities. Specialized "graded elements" have been shown to provide an efficient and accurate tool for the simulation of functionally graded materials. Most of the previous research on numerical simulation of functionally graded materials has been limited to elastic material behavior. Thus, the current work focuses on finite-element analysis of functionally graded viscoelastic materials. The analysis is performed using the elastic-viscoelastic correspondence principle, and viscoelastic material gradation is accounted for within the elements by means of the generalized iso-parametric formulation. This paper emphasizes viscoelastic behavior of asphalt concrete pavements and several examples, ranging from verification problems to field scale applications, are presented to demonstrate the features of the present approach.

Introduction

Functionally Graded Materials (FGMs) are characterized by spatially varied microstructures created by nonuniform distributions of the reinforcement phase with different properties, sizes and shapes, as well as, by interchanging the role of reinforcement and matrix materials in a continuous manner (Suresh and Mortensen 1998). They are usually engineered to produce property gradients aimed at optimizing structural response under different types of loading conditions (thermal, mechanical, electrical, optical, etc.) (Cavalcante et al. 2007). These property gradients are produced in several ways, for example by gradual variation of the content of one phase (ceramic) relative to another (metallic), as used in thermal barrier coatings, or by using a sufficiently large number of constituent phases with different properties (Miyamoto et al. 1999). Designer viscoelastic FGMs (VFGMs) can be tailored to meet design requirements such as viscoelastic columns subjected to axial and thermal loads (Hilton 2005). Recently, Muliana (2009) presented a micromechanical model for thermoviscoelastic behavior of FGMs.

Apart from engineered or tailored FGMs, several civil engineering materials naturally exhibit graded material properties. Silva et al. (2006) have studied and simulated bamboo, which is a naturally occurring graded material. Apart from natural occurrence, a variety of materials and structures exhibit nonhomogeneous material distribution and constitutive property gradations as an outcome of manufacturing or construction practices, aging, different amount of exposure to deteriorating agents, etc. Asphalt concrete pavements are one such example, whereby aging and temperature variation yield continuously graded nonhomogeneous constitutive properties. The aging and temperature induced property gradients have been well documented by several researchers in the field of asphalt pavements (Garrick 1995; Mirza and Witczak 1996; Apeagyei 2006; Chiasson et al. 2008). The current state-of-the-art in viscoelastic simulation of asphalt pavements is limited to either ignoring non-homogeneous property gradients (Kim and Buttlar 2002; Saad et al. 2006; Baek and Al-Qadi 2006; Dave et al. 2007) or considering them through a layered approach, for instance, the model used in the American Association of State Highway and Transportation Officials (AASHTO) Mechanistic Empirical Pavement Design Guide (MEPDG) (ARA Inc., EC. 2002). Significant loss of accuracy from the use of the layered approach for elastic analysis of asphalt pavements has been demonstrated (Buttlar et al. 2006).

Extensive research has been carried out to efficiently and accurately simulate functionally graded materials. For example, Cavalcante et al. (2007), Zhang and Paulino (2007), Arciniega and Reddy (2007), and Song and Paulino (2006) have all reported on finite-element simulations of FGMs. However, most of the previous research has been limited to elastic material behavior. A variety of civil engineering materials such as polymers, asphalt concrete, Portland cement concrete, etc., exhibit significant rate and history effects. Accurate simulation of these types of materials necessitates the use of viscoelastic constitutive models.

[1]Postdoctoral Research Associate, Dept. of Civil and Environmental Engineering, Univ. of Illinois at Urbana-Champaign, Urbana, IL 61801 (corresponding author).

[2]Donald Biggar Willett Professor of Engineering, Dept. of Civil and Environmental Engineering, Univ. of Illinois at Urbana-Champaign, Urbana, IL 61801.

[3]Professor and Narbey Khachaturian Faculty Scholar, Dept. of Civil and Environmental Engineering, Univ. of Illinois at Urbana-Champaign, Urbana, IL 61801.

The current work presents a finite element (FE) formulation tailored for analysis of viscoelastic FGMs and in particular, asphalt concrete. Paulino and Jin (2001) have explored the elastic-viscoelastic correspondence principle (CP) in the context of FGMs. The CP-based formulation has been used in the current study in conjunction with the generalized iso-parametric formulation (GIF) by Kim and Paulino (2002). This paper presents the details of the finite-element formulation, verification, and an asphalt pavement simulation example. Apart from simulation of asphalt pavements, the present approach could also be used for analysis of other engineering systems that exhibit graded viscoelastic behavior. Examples of such systems include metals and metal composites at high temperatures (Billotte et al. 2006; Koric and Thomas 2008); polymeric and plastic based systems that undergo oxidative and/or ultraviolet hardening (Hollaender et al. 1995; Hale et al. 1997) and graded fiber reinforced cement and concrete structures. Other application areas for the graded viscoelastic analysis include accurate simulation of the interfaces between viscoelastic materials such as the layer interface between different asphalt concrete lifts or simulations of viscoelastic gluing compounds used in the manufacture of layered composites (Diab and Wu 2007).

Functionally Graded Viscoelastic Finite-Element Method

This section describes the formulation for the analysis of viscoelastic functionally graded problems using FE framework and the elastic-viscoelastic CP. The initial portion of this section establishes the basic viscoelastic constitutive relationships and the CP. The subsequent section provides the FE formulation using the GIF.

Viscoelastic Constitutive Relations

The basic stress-strain relationships for viscoelastic materials have been presented by, among other writers, Hilton (1964) and Christensen (1982). The constitutive relationship for quasi-static, linear viscoelastic isotropic materials is given as

$$\sigma_{ij}(x,t) = 2\int_{t'=-\infty}^{t'=t} G[x,\xi(t)-\xi(t')]\left[\varepsilon_{ij}(x,t') - \frac{1}{3}\delta_{ij}\varepsilon_{kk}\right]dt'$$
$$+ \int_{t'=-\infty}^{t'=t} K[x,\xi(t)-\xi(t')]\delta_{ij}\varepsilon_{kk}dt' \qquad (1)$$

where σ_{ij}=stresses; ε_{ij}=strains at any location x. The parameters G and K=shear and bulk relaxation moduli; δ_{ij}=Kronecker delta; and t'=integration variable. Subscripts $(i,j,k,l=1,2,3)$ follow Einstein's summation convention. The reduced time ξ is related to real time t and temperature T through the time-temperature superposition principle

$$\xi(t) = \int_0^t a[T(t')]dt' \qquad (2)$$

For a nonhomogeneous viscoelastic body in quasi-static condition, assume a boundary value problem with displacement u_i on volume Ω_u, traction P_i on surface Ω_σ and body force F_i, the equilibrium and strain-displacement relationships (for small deformations) are as shown in Eq. (3)

$$\sigma_{ij,j} + F_i = 0, \quad \varepsilon_{ij} = \frac{1}{2}(u_{i,j}+u_{j,i}) \qquad (3)$$

respectively, where, u_i=displacement and $(\bullet)_{,j}=\partial(\bullet)/\partial x_j$.

CP and Its Application to FGMs

The CP allows a viscoelastic solution to be readily obtained by simple substitution into an existing elastic solution, such as a beam in bending, etc. The concept of equivalency between transformed viscoelastic and elastic boundary value problems can be found in Read (1950). This technique been extensively used by researchers to analyze variety of nonhomogeneous viscoelastic problems including, but not limited to, beam theory (Hilton and Piechocki 1962), finite-element analysis (Hilton and Yi 1993), and boundary element analysis (Sladek et al. 2006).

The CP can be more clearly explained by means of an example. For a simple one-dimensional (1D) problem, the stress-strain relationship for viscoelastic material is given by convolution integral shown in Eq. (4).

$$\sigma(t) = \int_0^t E(t-t')\frac{\partial\varepsilon(t')}{\partial t'}dt' \qquad (4)$$

If one is interested in solving for the stress and material properties and imposed strain conditions are known, using the elastic-viscoelastic correspondence principle the convolution integral can be reduced to the following relationship using an integral transform such as the Laplace transform:

$$\tilde{\sigma}(s) = s\tilde{E}(s)\tilde{\varepsilon}(s) \qquad (5)$$

Notice that the above functional form is similar to that of the elastic problem, thus the analytical solution available for elastic problems can be directly applied to the viscoelastic problem. The transformed stress quantity, $\tilde{\sigma}(s)$ is solved with known $\tilde{E}(s)$ and $\tilde{\varepsilon}(s)$. Inverse transformation of $\tilde{\sigma}(s)$ provides the stress $\sigma(t)$.

Mukherjee and Paulino (2003) have demonstrated limitations on the use of the correspondence principle in the context of functionally graded (and nonhomogenous) viscoelastic boundary value problems. Their work establishes the limitation on the functional form of the constitutive properties for successful and proper use of the CP.

Using correspondence principle, one obtains the Laplace transform of the stress-strain relationship described in Eq. (1) as

$$\tilde{\sigma}_{ij}(x,s) = 2\tilde{G}[x,\tilde{\xi}(s)]\tilde{\varepsilon}_{ij}(x,s) + \tilde{K}[x,\tilde{\xi}(s)]\delta_{ij}\tilde{\varepsilon}_{kk}(x,s) \qquad (6)$$

where s=transformation variable and the symbol tilde ($\sim$) on top of the variables represents transformed variable. The Laplace transform of any function $f(t)$ is given by

$$L[f(t)] = \tilde{f}(s) = \int_0^\infty f(t)Exp[-st]dt \qquad (7)$$

Equilibrium [Eq. (3)] for the boundary value problem in the transformed form becomes

$$\tilde{\sigma}_{,j}(x,s) = 2\tilde{G}(x,s)\tilde{\varepsilon}^d_{,j}(x,s) + 2\tilde{G}_{,j}(x,s)\tilde{\varepsilon}^d(x,s) + \tilde{K}(x,s)\tilde{\varepsilon}_{,j}(x,s)$$
$$+ \tilde{K}_{,j}(x,s)\tilde{\varepsilon}(x,s) \qquad (8)$$

where superscript d indicates the deviatoric component of the quantities.

Notice that the transformed equilibrium equation for a nonhomogeneous viscoelastic problem has identical form as an elastic

nonhomogeneous boundary value problem. This forms the basis for using CP-based FEM for solving graded viscoelastic problems such as asphalt concrete pavements. The basic FE framework for solving elastic problems can be readily used through the use of CP, which makes it an attractive alternative when compared to more involved time integration schemes. However, note that due to the inapplicability of the CP for problems involving the use of the time-temperature superposition principle, the present analysis is applicable to problems with nontransient thermal conditions. In the context of pavement analysis, this makes the present procedure applicable to simulation of traffic (tire) loading conditions for given aging levels. The present approach is not well-suited for thermal-cracking simulations, which require simulation of continuously changing and nonuniform temperature conditions.

FE Formulation

The variational principle for quasi-static linear viscoelastic materials under isothermal conditions can be found in Gurtin (1963). Taylor et al. (1970) extended it for thermoviscoelastic boundary value problem

$$
\begin{aligned}
\prod = {}& \int_{\Omega_u} \int_{t'=-\infty}^{t'=t} \int_{t''=-\infty}^{t''=t-t'} \frac{1}{2} C_{ijkl}[x, \xi_{ijkl}(t-t'') - \xi'_{ijkl}(t')] \\
& \times \frac{\partial \varepsilon_{ij}(x,t')}{\partial t'} \frac{\partial \varepsilon_{kl}(x,t'')}{\partial t''} dt' dt'' d\Omega_u \\
& - \int_{\Omega_u} \int_{t'=-\infty}^{t'=t} \int_{t''=-\infty}^{t''=t-t'} C_{ijkl}[x, \xi_{ijkl}(t-t'') - \xi'_{ijkl}(t')] \\
& \times \frac{\partial \varepsilon^*_{ij}(x,t')}{\partial t'} \frac{\partial \varepsilon^*_{kl}(x,t'')}{\partial t''} dt' dt'' d\Omega_u \\
& - \int_{\Omega_\sigma} \int_{t''=-\infty}^{t''=t} P_i(x,t-t'') \frac{\partial u_i(x,t'')}{\partial t''} dt'' d\Omega_\sigma = 0
\end{aligned}
\tag{9}
$$

where Ω_u=volume of a body; Ω_σ=surface on which tractions P_i are prescribed; u_i=displacements; C_{ijkl}=space and time dependent material constitutive properties; ε_{ij}=mechanical strains and ε^*_{ij}=thermal strains; while ξ_{ijkl}=reduced time related to real time t and temperature T through time-temperature superposition principle of Eq. (2).

The first variation provides the basis for the FE formulation

$$
\begin{aligned}
\delta \prod = {}& \int_{\Omega_u} \int_{t'=-\infty}^{t'=t} \int_{t''=-\infty}^{t''=t-t'} \left\{ C_{ijkl}[x, \xi_{ijkl}(t-t'') - \xi'_{ijkl}(t')] \frac{\partial}{\partial t'} (\varepsilon_{ij}(x,t') \right. \\
& \left. - \varepsilon^*_{ij}(x,t')) \frac{\partial \delta \varepsilon_{kl}(x,t'')}{\partial t''} \right\} dt' dt'' d\Omega_u \\
& - \int_{\Omega_\sigma} \int_{t''=-\infty}^{t''=t} P_i(x,t-t'') \frac{\partial \delta u_i(x,t'')}{\partial t''} dt'' d\Omega_\sigma = 0
\end{aligned}
\tag{10}
$$

The element displacement vector u_i is related to nodal displacement degrees of freedom q_j through the shape functions N_{ij}

$$
u_i(x,t) = N_{ij}(x) q_j(t)
\tag{11}
$$

Differentiation of Eq. (11) yields the relationship between strain ε_i and nodal displacements q_i through derivatives of shape functions B_{ij}

$$
\varepsilon_i(x,t) = B_{ij}(x) q_j(t)
\tag{12}
$$

Eqs. (10)–(12) provide the equilibrium equation for each finite element

$$
\int_0^t k_{ij}[x, \xi(t) - \xi(t')] \frac{\partial q_j(t')}{\partial t'} dt' = f_i(x,t) + f_i^{th}(x,t)
\tag{13}
$$

where k_{ij}=element stiffness matrix; f_i=mechanical force vector; and f_i^{th}=thermal force vector, which are described as follows:

$$
k_{ij}(x,t) = \int_{\Omega_u} B_{ik}^T(x) C_{kl}[x, \xi(t)] B_{lj}(x) d\Omega_u
\tag{14}
$$

$$
f_i(x,t) = \int_{\Omega_\sigma} N_{ij}(x) P_j(x,t) d\Omega_\sigma
\tag{15}
$$

$$
f_i^{th}(x,t) = \int_{\Omega_u} \int_{-\infty}^t B_{ik}(x) C_{kl}[x, \xi(t) - \xi(t')] \frac{\partial \varepsilon_l^*(x,t')}{\partial t'} dt' d\Omega_u
\tag{16}
$$

$$
\varepsilon_l^*(x,t) = \alpha(x) \Delta_T(x,t)
\tag{17}
$$

where α=coefficient of thermal expansion and Δ_T=temperature change with respect to initial conditions.

On assembly of the individual finite element contributions for the given problem domain, the global equilibrium equation can be obtained as

$$
\int_0^t K_{ij}[x, \xi(t) - \xi(t')] \frac{\partial U_j(t')}{\partial t'} dt' = F_i(x,t) + F_i^{th}(x,t)
\tag{18}
$$

where K_{ij}=global stiffness matrix; U_i=global displacement vector; and F_i and F_i^{th}=global mechanical and thermal force vectors respectively. The solution to the problem requires solving the convolution shown above to determine nodal displacements.

Hilton and Yi (1993) have used the CP-based procedure for implementing the FE formulation. However, the previous research efforts were limited to use of conventional finite elements, while in the current paper graded finite elements have been used to efficiently and accurately capture the effects of material nonhomogeneities. Graded elements have benefit over conventional elements in context of simulating non-homogeneous isotropic and orthotropic materials (Paulino and Kim 2007). Kim and Paulino (2002) proposed graded elements with the GIF, where the constitutive material properties are sampled at each nodal point and interpolated back to the Gauss-quadrature points (Gaussian integration points) using isoparametric shape functions. This type of formulation allows for capturing the material nonhomogeneities within the elements unlike conventional elements which are homogeneous in nature. The material properties, such as shear modulus, are interpolated as

$$
G_{\text{Int. Point}} = \sum_{i=1}^m G_i N_i
\tag{19}
$$

where N_i=shape functions; G_i=shear modulus corresponding to node i; and m=number of nodal points in the element.
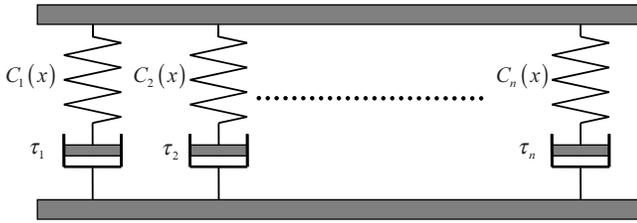
Fig. 1. Generalized Maxwell model

Fig. 2. Outline of finite-element analysis procedure

A series of weak patch tests for the graded elements have been previously established (Paulino and Kim 2007). This work demonstrated the existence of two length scales: (1) length scale associated with element size, and (2) length scale associated with material nonhomogeneity. Consideration of both length scales is necessary in order to ensure convergence. Other uses of graded elements include evaluation of stress-intensity factors in FGMs under mode I thermomechanical loading (Walters et al. 2004), and dynamic analysis of graded beams (Zhang and Paulino 2007), which also illustrated the use of graded elements for simulation of interface between different material layers. In a recent study (Silva et al. 2007) graded elements were extended for multiphysics applications.

Using the elastic-viscoelastic CP, the functionally graded viscoelastic finite element problem could be deduced to have a functional form similar to that of elastic problems. Laplace transform of the global equilibrium shown in Eq. (18) is

$$\widetilde{K}_{ij}(x,s)\widetilde{U}_j(s) = \widetilde{F}_i(x,s) + \widetilde{F}_i^{th}(x,s) \qquad (20)$$

Notice that the Laplace transform of hereditary integral [Eq. (18)] led to an algebraic relationship [Eq. (23)], this is major benefit of using CP as the direct integration for solving hereditary integrals will have significant computational cost. As discussed in a previous section, the applicability of correspondence principle for viscoelastic FGMs imposes limitations on the functional form of constitutive model. With this knowledge, it is possible to further customize the FE formulation for the generalized Maxwell model. Material constitutive properties for generalized Maxwell model is given as

$$C_{ij}(x,t) = \sum_{h=1}^{n} \left[C_{ij}(x) \right]_h Exp\left[-\frac{t}{(\tau_{ij})_h} \right] \quad \text{(no sum)} \qquad (21)$$

where $(C_{ij})_h$=elastic contributions (spring coefficients); $(\tau_{ij})_h$ =viscous contributions from individual Maxwell units, commonly called relaxation times; and n=number of Maxwell unit.

Fig. 1 illustrates simplified 1D form of the generalized Maxwell model represented in Eq. (21). Notice that the generalized Maxwell model discussed herein follows the recommendations made by Mukherjee and Paulino (2003) for ensuring success of the correspondence principle.

For the generalized Maxwell model, the global stiffness matrix K of the system can be rewritten as

$$K_{ij}(x,t) = K_{ij}^0(x) Exp\left(-\frac{t}{\tau_{ij}} \right) = K_{ij}^0(x) K_{ij}^t(t) \quad \text{(no sum)} \qquad (22)$$

where K_{ij}^0=elastic contribution of stiffness matrix and K^t=time dependent portion.

Using Eqs. (20) and (22), one can summarize the problem as

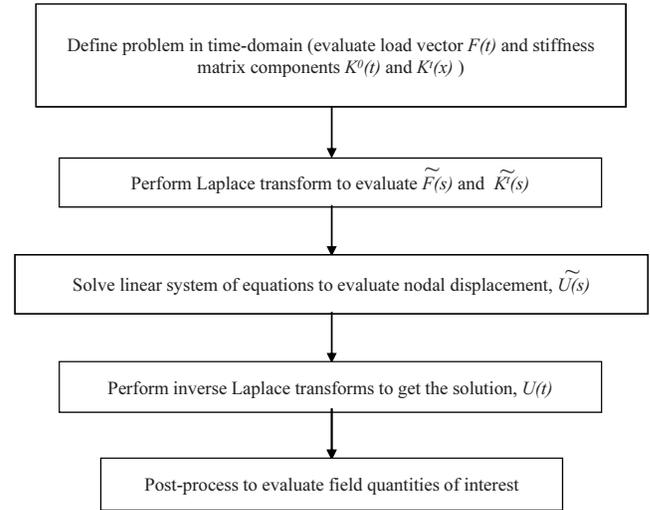$$K_{ij}^0(x)\widetilde{K}_{ij}^t(s)\widetilde{U}_j(s) = \widetilde{F}_i(x,s) + \widetilde{F}_i^{th}(x,s) \quad \text{(no sum)} \qquad (23)$$

FE Implementation

The FE formulation described in the previous section was implemented and applied to two-dimensional plane and axisymmetric problems. This section provides the details of the implementation of formulation along with brief description method chosen for numerical inversion from Laplace domain to time domain.

The implementation was coded in the commercially available software Matlab. The implementation of the analysis code is divided into five major steps as shown in Fig. 2.

The first step is very similar to the FE method for a time dependent nonhomogeneous problem, whereby local contributions from various elements are assembled to obtain the force vector and stiffness matrix for the system. Notice that due to the time dependent nature of the problem the quantities are evaluated throughout the time duration of analysis. The next step is to transform the quantities to the Laplace domain from the time domain. For the generalized Maxwell model, the Laplace transform of the time-dependent portion of the stiffness matrix, K^t, can be directly (and exactly) determined using the analytical transform given by

$$K_{ij}^0(x)\widetilde{K}_{ij}^t(s)\widetilde{U}_j(s) = \widetilde{F}_i(x,s) + \widetilde{F}_i^{th}(x,s) \quad [\text{no sum for } K_{ij}^0(x)\widetilde{K}_{ij}^t(s)]$$

$$(24)$$

Laplace transform of quantities other than the stiffness matrix can be evaluated using the trapezoidal rule, assuming that the quantities are piecewise linear functions of time. Thus, for a given time dependent function $F(t)$, the Laplace transform $\widetilde{F}(s)$ is estimated as

$$\widetilde{F}(s) = \sum_{i=1}^{N-1} \frac{1}{s^2 \Delta t} \{ s\Delta t (F(t_i)Exp[-st_i] - F(t_{i+1})Exp[-st_{i+1}])$$

$$+ \Delta F(Exp[-st_i] - Exp[-st_{i+1}]) \} \qquad (25)$$

where Δt=time increment; N=total number of increments; and ΔF=change in function F for the given increment.

Once the quantities are calculated on the transformed domain the system of linear equations are solved to determine the solution, which in this case produces the nodal displacements in the transformed domain, $\widetilde{U}(s)$. The inverse transform provides the solution to the problem in the time domain. It should be noted that
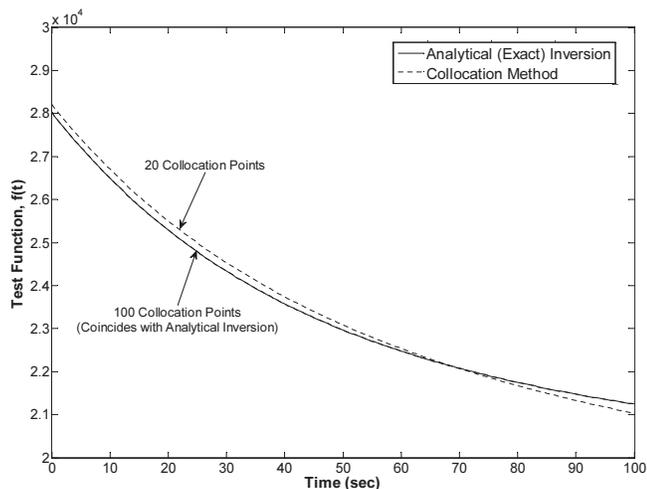
Fig. 3. Numerical Laplace inversion using collocation method

Fig. 4. Comparison of exact (line) and numerical solution (circular markers) for bending of FGM bar (insert illustrates the boundary value problem along with material gradation)

the formulation as well as its implementation is relatively straight forward using the correspondence principle based transformed approach when compared to numerically solving the convolution integral.

The inverse Laplace transform is of greater importance in the current problem as the problem is ill posed due to absence of a functional description in the imaginary plane. Comprehensive comparisons of various numerical inversion techniques have been previously presented (Beskos and Narayanan 1983). In the current study, the collocation method (Schapery 1962; Schapery 1965) was used on basis of the recommendations from previous work (Beskos and Narayanan 1983; Yi 1992).

For the current implementation the numerical inverse transform is compared with exact inversion using generalized Maxwell model [c.f. Eq. (21)] as the test function. The results, shown in Fig. 3, compare the exact analytical inversion with the numerical inversion results. The numerical inversion was carried out using 20 and 100 collocation points. With 20 collocation points, the average relative error in the numerical estimate is 2.7%, whereas with 100 collocation points, the numerical estimate approaches the exact inversion.

Verification Examples

In order to verify the present formulation and its implementation, a series of verifications were performed. The verification was divided into two categories: (1) verification of the implementation of GIF elements to capture material nonhomogeneity, and (2) verification of the viscoelastic portion of the formulation to capture time and history dependent material response.

Verification of Graded Elements

A series of analyzes were performed to verify the implementation of the graded elements. The verifications were performed for fixed grip, tension and bending (moment) loading conditions. The material properties were assumed to be elastic with exponential spatial variation. The numerical results were compared with exact analytical solutions available in the literature (Kim and Paulino 2002). The comparison results for fixed grip loading, tensile loading, and bending were performed. The results for all three cases
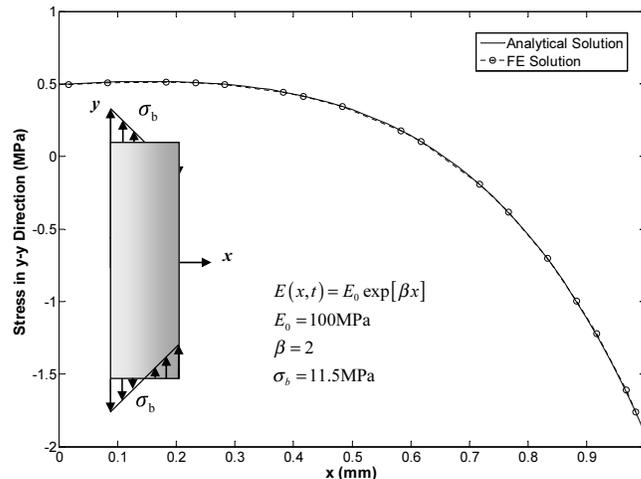
show a very close match with the analytical solution verifying the implementation of the GIF graded elements. Comparison for the bending case is presented in Fig. 4.

Verification of Viscoelastic Analysis

Verification results for the implementation of the correspondence principle based viscoelastic functionally graded analysis were performed and are provided. The first verification example represents a functionally graded viscoelastic bar undergoing creep deformation under a constant load. The analysis was conducted for the Maxwell model. Fig. 5 compares analytical and numerical results for this verification problem. The analytical solution (Mukherjee and Paulino 2003) was used for this analysis. It can be observed that the numerical results are in very good agreement with the analytical solution.

The second verification example was simulated for fixed grip loading of an exponentially graded viscoelastic bar. The numerical results were compared with the available analytical solution
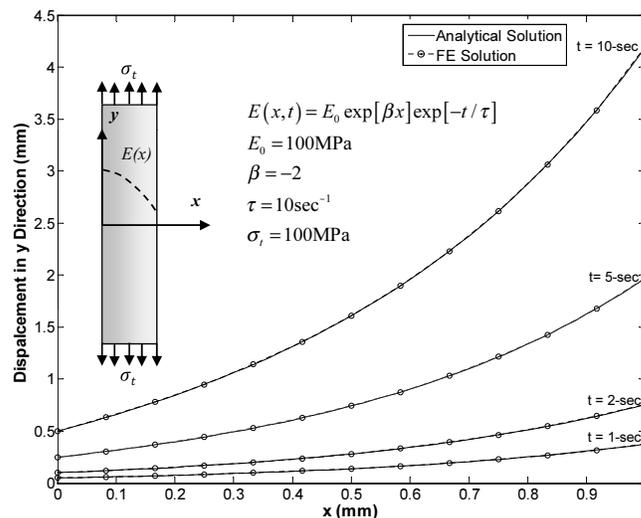

Fig. 5. Comparison of exact and numerical solution for the creep of exponentially graded viscoelastic bar
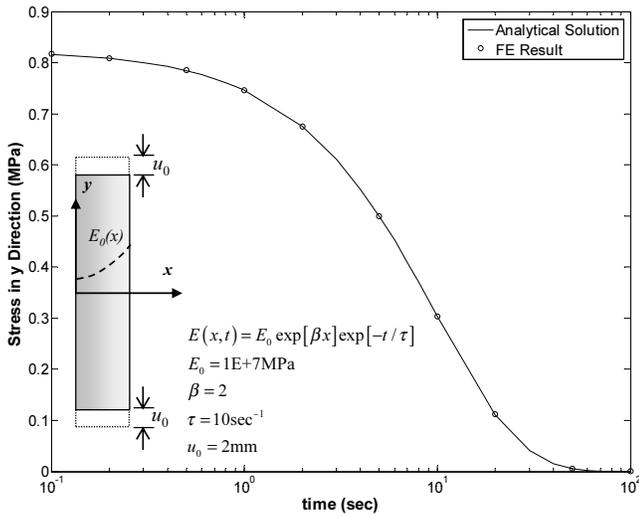
Fig. 6. Comparison of exact and numerical solution for the exponentially graded viscoelastic bar in fixed grip loading

(Mukherjee and Paulino 2003) for a viscoelastic FGM. Fig. 6 compares analytical and numerical results for this verification problem. Notice that the results are presented as function of time, and in this boundary value problem the stresses in y-direction are constant over the width of bar. Excellent agreement between numerical results and analytical solution further verifies the veracity of the viscoelastic graded FE formulation derived herein and its successful implementation.

Application Examples

In this section, two sets of simulation examples using the graded viscoelastic analysis scheme discussed in this paper are presented. The first example is for a simply supported functionally graded viscoelastic beam in a three-point bending configuration. In order to demonstrate the benefits of the graded analysis approach, comparisons are made with analysis performed using commercially available software (ABAQUS). In the case, of ABAQUS simulations, the material gradation is approximated using a layered approach and different refinement levels. The second example is that of an aged conventional asphalt concrete pavement loaded with a truck tire.

Simply Supported Graded Viscoelastic Beam

Fig. 7 shows the geometry and boundary conditions for the graded viscoelastic simply supported beam. A creep load, $P(t)$, is imposed at midspan
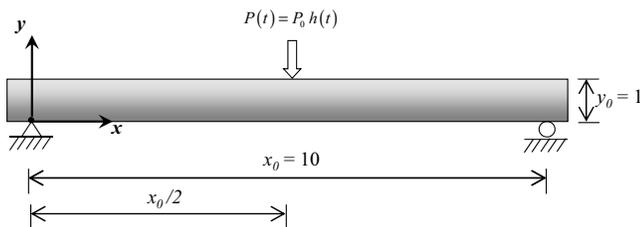

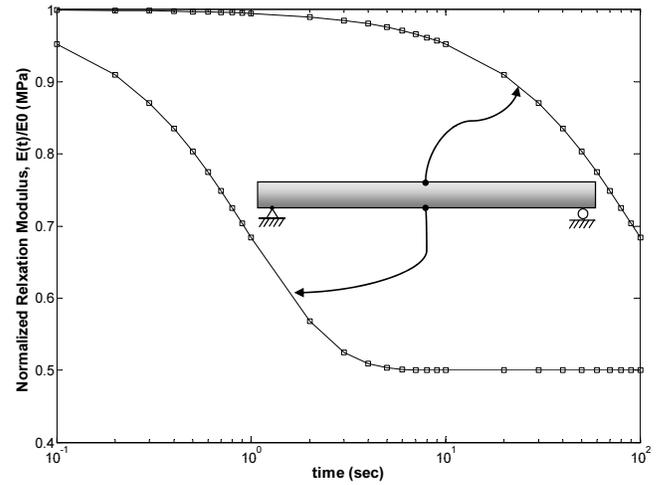**Fig. 7.** Graded viscoelastic beam problem configuration

Fig. 8. Relaxation moduli on top and bottom of the graded beam

$$P(t) = P_0 t \qquad (26)$$

The viscoelastic relaxation moduli on the top ($y = y_0$) and bottom ($y = 0$) of the beam are shown in Fig. 8. The variation of moduli is assumed to vary linearly from top to bottom as follows:

$$E(y,t) = \left(\frac{y}{y_0}\right) E_{\text{Top}}(t) + \left(\frac{y_0 - y}{y_0}\right) E_{\text{Bottom}}(t) \qquad (27)$$

The problem was solved using three approaches namely, (1) graded viscoelastic analysis procedure (present paper); (2) commercial software ABAQUS with different levels of mesh refinements and averaged material properties assigned in the layered manner; and (3) assuming averaged material properties for the whole beam. In the case of the layered approach using commercial software ABAQUS, three levels of discretization were used. A sample of the mesh discritization used for each of the simulation cases is shown in Fig. 9. Table 1 presents mesh attributes for each of the simulation cases.

The parameter selected for comparing the various analysis options is the mid span deflection for the beam problem discussed earlier (c.f. Fig. 7). The results from all four simulation options are presented in Fig. 10. Due to the viscoelastic nature of the problem, the beam continues to undergo creep deformation with increasing loading time. The results further illustrate the benefit of using the graded analysis approach as a finer level of mesh
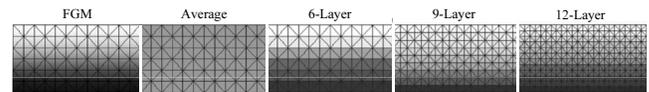

Fig. 9. Mesh discretization for various simulation cases (1/5th beam span shown for each case)

Table 1. Mesh Attributes for Different Analysis Options

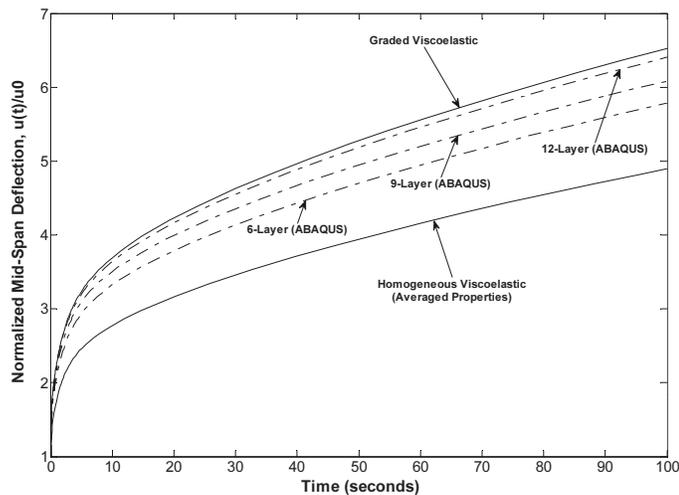| Simulation case	Number of elements	Number of nodes	Total degrees of freedom
FGM/average/6-layer	720	1,573	3,146
9-layer	1,620	3,439	6,878
12-layer	2,880	6,025	12,050

Fig. 10. Normalized midspan deflection for the beam

refinement is required in order for the layered approach to begin to converge with the graded approach. The results also demonstrate the drawback of using averaged properties which yield significantly poorer results when compared to graded and layered approaches. Also, it is worthy to note that in the case of graded viscoelastic problems, it is important to consider the results over the complete time history. In the current problem, the severity of the material gradation increases with time. This effect is apparent in the results, where the deviation between graded and layered approaches increases with increasing time.

Aged Conventional Asphalt Concrete Pavement

An asphalt pavement simulation example is presented in this section to illustrate the application of the graded viscoelastic FE analysis procedure. The simulation was also conducted for the same problem using the layered approach, and results from layered and graded approaches are compared. A conventional asphalt pavement section was simulated. Section details are shown in Fig. 11 along with the FE mesh.

The pavement was assumed to be highly aged, and hence the asphalt concrete layer was simulated as a graded viscoelastic ma-
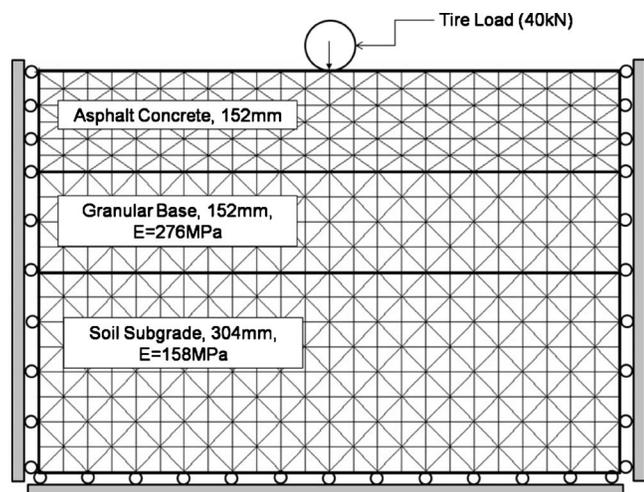
terial. Apeagyei et al. (2006; 2008) have recently studied the effects of antioxidant treatment on asphalt binders and mixtures. They have performed viscoelastic characterization of short-term and long-term aged asphalt mixtures. Short term and long-term aged properties from Apeagyei et al. 2008 were used for simulation of aged asphalt concrete pavement in this example. The shear relaxation modulus is assumed to be varying linearly through the pavement thickness, going from a long-term aged condition on surface to a short-term aged condition on the bottom of the asphalt concrete layer. This is illustrated in Fig. 12. The bulk modulus is assumed to be constant with time. In the case of the layered simulation, the asphalt concrete layer was divided into six layers, where each layer was assigned average properties.

Boundary conditions for the simulation problem are given in Fig. 11. The imposed load was applied to simulate a single 40 kN (9,000 lb) tire with 700 kPa (100 psi) pressure. Contact pressure was assumed to be vertically oriented (no horizontal loading). The asphalt concrete temperature was assumed to be uniform through the thickness, with value of −10°C.

In the case of asphalt pavements, stresses in the horizontal direction are often of interest to the pavement engineer, as they are taken as critical response parameters at low and intermediate temperatures. These stresses are commonly linked to fatigue cracking in pavements, which is one of the most devastating pavement damage mechanisms. The horizontal stresses directly under the tire load are compared for layered and graded viscoelastic approaches. The results are shown in Fig. 13 for stresses at a loading time of 100 s. Notice that in order to exaggerate the difference between layered and graded approaches, the nodal stresses are presented for the graded approach, whereas for the layered approach, the nodal stresses are averaged in a layered fashion. Hence, the discontinuities are observed at layer interfaces. It is interesting to note that the extent of tensile stresses is relatively low as compared to the compressive stresses near the surface. This trend is not unexpected for the aged pavement system, as the material closer to surface is stiffer, and thus accumulates greater stresses, while unaged material near the bottom is compliant and exhibits a greater degree of stress relaxation.

Summary, Conclusions, and Future Directions

A functionally graded viscoelastic FE formulation based on correspondence principle has been proposed. The formulation is implemented to solve 2D plane and axisymmetric problems. The GIF has been extended for graded (nonhomogeneous) viscoelastic elements. The collocation method was selected for performing the inverse Laplace transformation. The implementation has been verified for cases involving material nonhomogeneities as well as viscoelastic effects.

Two application examples were presented. The first example provided a comparison between graded, averaged homogeneous and layered approaches. Also, a comparison between the predictions made using the present approach versus those made by commercially available software was provided. A second example was provided to illustrate responses for an aged graded asphalt concrete pavement system.

Based on the findings from this study following conclusions could be drawn:

1. The FE framework for solving nonhomogeneous viscoelastic problems is very similar to non-homogeneous elastic problems when developed using CP-based formulation.
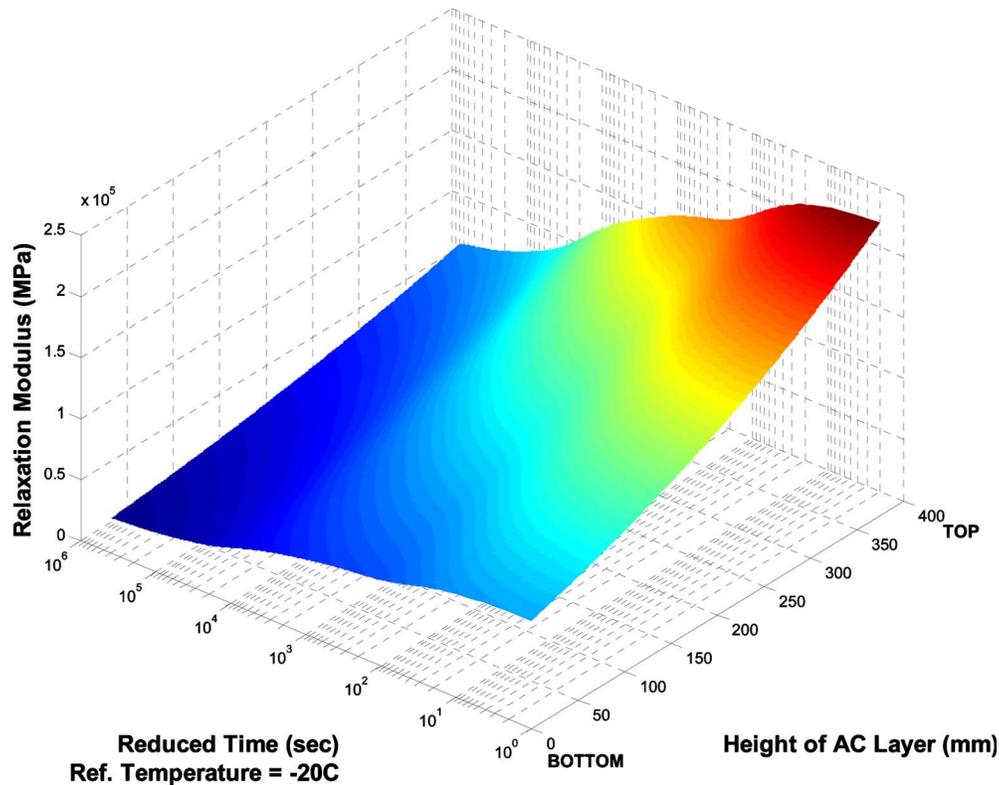

Fig. 11. Pavement section and FE mesh for simulation example

Fig. 12. Relaxation modulus of asphalt concrete (variation with depth and time)

2. The graded viscoelastic analysis proposed herein yields significant accuracy benefits over the layered analysis, but with the same computational cost. More accurate results with a coarser mesh were obtained using the graded viscoelastic approach, which will be of particular benefit for larger simulations, particularly when extending the approach to 3D.

3. Response predictions at layer interfaces will be unrealistic when using layered analysis approaches for nonhomogeneous viscoelastic problems. Application of graded analysis technique circumvents this issue. This is of particular interest when trying to simulate the interface conditions between the asphalt layers.

Fig. 13. Stresses in horizontal direction (x-direction) directly under the tire load

4. For viscoelastic graded systems, the predictions from layered systems may impose a varying degree of inaccuracy with time. This makes it difficult to predict the degree of error in layered approximation, thus further reinforcing benefits of using a graded viscoelastic analysis procedure, such as the one developed herein.

During the course of this study, the following future directions were identified:

1. The technique developed here should be extended to 3D analysis. This is particularly important to obtain realistic pavement responses from complex and combined tire loadings.

2. The present research should be applied for realistic simulation of the layer interface conditions. The effects of graded interfaces on pavement performance prediction should be studied.

3. The present analysis technique should be used to evaluate a variety of aged asphalt pavement and overlay systems and to study pavement distresses, such as thermal, reflective and topdown cracking.

4. The current analysis procedure should be integrated with asphalt aging models to study performance variation of asphalt pavements during the course of service life.

5. The approach presented herein should be used in conjunction with comprehensive field studies to validate its benefits over the currently available layered analysis and design approach.

6. The present formulation is applicable to static temperature conditions due to the inapplicability of the correspondence principle for problems involving the time-temperature superposition principle. Other techniques, such as time-integration formulations, should be studied to develop techniques capable of simulating transient and nonuniform temperature conditions.
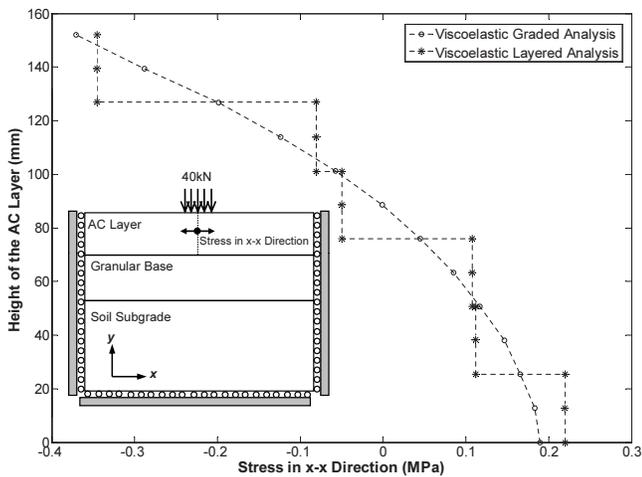
Acknowledgments

References

Apeagyei, A. K. (2006). "Antioxidant treatment for asphalt binders and mixtures." Ph.D. thesis, Univ. of Illinois at Urbana-Champaign, Urbana, Ill.

Apeagyei, A. K., Buttlar, W. G., and Dempsey, B. J. (2008). "Investigation of cracking behavior of antioxidant-modified asphalt mixtures." *J. Asph. Paving Technol.*, 77, 393–430.

ARA Inc, EC. (2002). "Guide for Mechanistic-Empirical Design of New and Rehabilitated Pavement Structures." *Rep. Project No. NCHRP 1–37A Final Rep.*, National Cooperative Highway Research Program, Washington, D.C.

Arciniega, R. A., and Reddy, J. N. (2007). "Large deformation analysis of functionally graded shells." *Int. J. Solids Struct.*, 44(6), 2036–2052.

Baek, J., and Al-Qadi, I. L. (2006). "Finite-element method modeling of reflective cracking initiation and propagation: Investigation of the effect of steel reinforcement interlayer on retarding reflective cracking in hot-mix asphalt overlay." *Transp. Res. Rec.*, 1949, 32–42.

Beskos, D. E., and Narayanan, G. V. (1983). "Dynamic response of frameworks by numerical Laplace transform." *Comput. Methods Appl. Mech. Eng.*, 37(3), 289–307.

Billotte, C., Carreau, P. J., and Heuzey, M. C. (2006). "Rheological characterization of a solder paste for surface mount applications." *Rheol. Acta (Germany)*, 45(4), 374.

Buttlar, W. G., Paulino, G. H., and Song, S. H. (2006). "Application of graded finite elements for asphalt pavements." *J. Eng. Mech.*, 132(3), 240–249.

Cavalcante, M. A. A., Marques, S. P. C., and Pindera, M. (2007). "Parametric formulation of the finite-volume theory for functionally graded materials. Part 1: Analysis." *J. Appl. Mech.*, 74(5), 935–945.

Chiasson, A. D., Yavuzturk, C., and Ksaibati, K. (2008). "Linearized approach for predicting thermal stresses in asphalt pavements due to environmental conditions." *J. Mater. Civ. Eng.*, 20(2), 118.

Christensen, R. M. (1982). *Theory of viscoelasticity*, Dover, Mineola, N.Y.

Dave, E. V., Song, S. H., Buttlar, W. G., and Paulino, G. H. (2007). "Reflective and thermal cracking modeling of asphalt concrete overlays." *Proc., Advance Characterization of Pavement and Soil Engineering Materials—2007*, Taylor and Francis, London, 1241–1252.

Diab, H., and Wu, Z. (2007). "Nonlinear constitutive model for time-dependent behavior of FRP-concrete interface." *Compos. Sci. Technol.*, 67(11–12), 2323.

Garrick, N. W. (1995). "Nonlinear differential equation for modeling asphalt aging." *J. Mater. Civ. Eng.*, 7(4), 265.

Gurtin, M. E. (1963). "Variational principles in the linear theory of viscoelasticity." *Arch. Ration. Mech. Anal.*, 13, 179–191.

Hale, G. D., Oldenburg, S. J., and Halas, N. J. (1997). "Effects of photo-oxidation on conjugated polymer films." *Appl. Phys. Lett.*, 71(11), 1483.

Hilton, H. H. (1964). *Viscoelastic analysis*, Engineering Design for Plastics, Reinhold, New York, 199.

Hilton, H. H. (2005). "Optimum linear and nonlinear viscoelastic designer functionally graded materials—Characterizations and analysis." *Composites, Part A*, 36(10), 1329–1334.

Hilton, H. H., and Piechocki, J. J. (1962). "Shear center motion in beams with temperature dependent linear elastic or viscoelastic properties." *Proc., 4th U.S. National Congress of Applied Mechanics*, American Society of Mechanical Engineers, New York, 1279–1289.

Hilton, H. H., and Yi, S. (1993). "Anisotropic viscoelastic finite element analysis of mechanically and hygrothermally loaded composites." *Composites Eng.*, 3(2), 123–135.

Hollaender, A., Klemberg-Sapieha, J. E., and Wertheimer, M. R. (1995). *Polymer oxidation induced by vacuum-ultraviolet emission*, Garmisch-Partenkirchen, Germany, 55.

Kim, J., and Buttlar, W. G. (2002). "Analysis of reflective crack control system involving reinforcing grid over based-isolating interlayer mixture." *J. Transp. Eng.*, 128(4), 375–384.

Kim, J., and Paulino, G. H. (2002). "Isoparametric graded finite elements for nonhomogeneous isotropic and orthotropic materials." *J. Appl. Mech.*, 69(4), 502–514.

Koric, S., and Thomas, B. G. (2008). "Thermo-mechanical models of steel solidification based on two elastic visco-plastic constitutive laws." *J. Mater. Process. Technol.*, 197(1–3), 408.

Mirza, M. W., and Witczak, M. W. (1996). "Development of a global aging system for short and long term aging of asphalt cements." *Proc., 1995 Conf. of the Association of Asphalt Paving Technologists*, Association of Asphalt Paving Technologists, Maplewood, Minn., 393–430.

Miyamoto, Y., Kaysser, W. A., Rabin, B. H., Kawasaki, A., and Ford, R. G. (1999). *Functionally graded materials: Design, processing, and applications*, Kluwer Academic, The Netherlands.

Mukherjee, S., and Paulino, G. H. (2003). "The elastic-viscoelastic correspondence principle for functionally graded materials, revisited." *J. Appl. Mech.*, 70(3), 359–363.

Muliana, A. H. (2009). "A micromechanical model for predicting thermal properties and thermo-viscoelastic responses of functionally graded materials." *Int. J. Solids Struct.*, 46(9), 1911–1924.

Paulino, G. H., and Jin, Z. (2001). "Correspondence principle in viscoelastic functionally graded materials." *J. Appl. Mech.*, 68(1), 129–132.

Paulino, G. H., and Kim, J. (2007). "The weak patch test for nonhomogeneous materials modeled with graded finite elements." *J. Braz. Soc. Mech. Sci. Eng.*, 29(1), 63–81.

Read, W. T., Jr. (1950). "Stress analysis for compressible viscoelastic materials." *J. Appl. Phys.*, 21, 671–674.

Saad, B., Mitri, H., and Poorooshasb, H. (2006). "3D FE analysis of flexible pavement with geosynthetic reinforcement." *J. Transp. Eng.*, 132(5), 402.

Schapery, R. A. (1962). "A note on approximate methods pertinent to thermo-viscoelastic stress analysis." *Report No. GALCIT SM 62–40*, California Institute of Technology, Pasadena, Calif.

Schapery, R. A. (1965). "Method of viscoelastic stress analysis using elastic solutions." *Franklin Institute—J.*, 279(4), 268–289.

Silva, E. C. N., Carbonari, R. C., and Paulino, G. H. (2007). "On graded elements for multiphysics applications." *Smart Mater. Struct.*, 16(6), 2408–2428.

Silva, E. C. N., Walters, M. C., and Paulino, G. H. (2006). "Modeling bamboo as a functionally graded material: Lessons for the analysis of affordable materials." *J. Mater. Sci.*, 41(21), 6991–7004.

Sladek, J., Sladek, V., Zhang, C., and Schanz, M. (2006). "Meshless local Petrov-Galerkin method for continuously nonhomogeneous linear viscoelastic solids." *Comput. Mech.*, 37(3), 279–289.

Song, S. H., and Paulino, G. H. (2006). "Dynamic stress intensity factors for homogeneous and smoothly heterogeneous materials using the interaction integral method." *Int. J. Solids Struct.*, 43(16), 4830–4866.

Suresh, S., and Mortensen, A. (1998). *Functionally graded materials*, Institute of Materials, IOM Communications, London.

Taylor, R. L., Pister, K. S., and Goudreau, G. L. (1970). "Thermomechanical analysis of viscoelastic solids." *Int. J. Numer. Methods Eng.*, 2(1), 45–59.

Walters, M. C., Paulino, G. H., and Dodds, R. H., Jr. (2004). "Stress-intensity factors for surface cracks in functionally graded materials under mode-1 thermomechanical loading." *Int. J. Solids Struct.*, 41(3–4), 1081–1118.

Yi, S. (1992). "Finite-element analysis of anisotropic viscoelastic composite structures and analytical determination of optimum viscoelastic material properties." Ph.D. thesis, Univ. of Illinois, Urbana, Ill.

Zhang, Z., and Paulino, G. H. (2007). "Wave propagation and dynamic analysis of smoothly graded heterogeneous continua using graded finite elements." *Int. J. Solids Struct.*, 44(11–12), 3601–3626.